



1 **The effects of Hurricane Harvey on Texas coastal zone chemistry**

2

3

Piers Chapman^{1,2}, Steven F. DiMarco^{1,2}, Anthony H. Knap^{1,2}, Antonietta Quigg^{1,3}, Nan D.
Walker⁴

4

5

6

1. Department of Oceanography, Texas A&M University, College Station, TX 77843

7

2. Geochemical and Environmental Research Group, Texas A&M University, College
Station, TX 77843

8

9

3. Department of Marine Biology, Texas A&M University, Galveston, TX 77553

10

4. Department of Oceanography and Coastal Sciences, Louisiana State University, Baton Rouge,
LA, 70803

11

12

13

Correspondence to: Piers Chapman (piers.chapman@tamu.edu)

14

15

Abstract

16

Hurricane Harvey deposited over 90 billion cubic meters of rainwater over central Texas, USA,

17

during late August/early September 2017. During four cruises (June, August, September and

18

November 2017) we observed changes in hydrography, nutrient and oxygen concentrations in

19

Texas coastal waters. Despite intense terrestrial runoff, nutrient supply to the coastal ocean was

20

transient, with little phytoplankton growth observed and no hypoxia. Observations suggest this

21

was probably related to the retention of nutrients in the coastal bays, rapid uptake by

22

phytoplankton of nutrients washed out of the bays, as well as dilution by the sheer volume of

23

rainwater, and the lack of significant carbon reserves in the sediments, despite the imposition of

24

a strong pycnocline. By the November cruise conditions had apparently returned to normal and

25

no long-term effects were observed.

26

27

Keywords

28

Hurricane Harvey, Texas coast, nutrients, oxygen, chlorophyll

29



30 **1. Introduction**

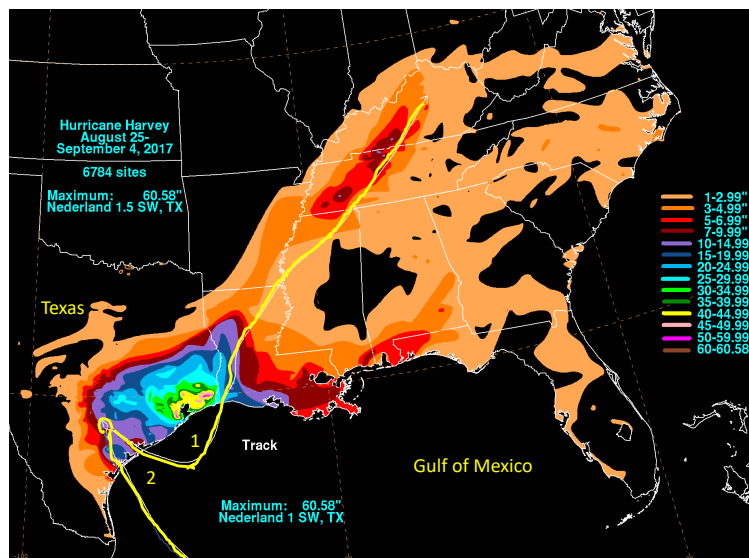
31 The Gulf of Mexico is renowned for its hurricanes and tropical storms, and the Galveston
32 hurricane of 1900, with an estimated total fatality of over 8,000, has the distinction of still being
33 the worst natural disaster in the U.S. in recorded history (Larson, 1999). More recently,
34 hurricanes such as Andrew (1992), Katrina, Rita and Wilma (2005), and Ike (2008) have ravaged
35 the northern Gulf coast, causing extensive damage and large financial losses. 2017 was another
36 active year in the Atlantic, with 10 hurricanes and 8 tropical cyclones and depressions, including
37 the category 5 hurricanes Irma, which affected several Caribbean islands and reached Florida as
38 a category 3 storm in late August/early September, and Maria, which devastated Dominica and
39 Puerto Rico in September (see the archives at <http://www.nhc.noaa.gov>).

40
41 Hurricane Harvey developed in the Bay of Campeche, in the extreme southwestern part of the
42 Gulf of Mexico, on 23 August, 2017, intensifying rapidly on August 24 over water with
43 SST $>30^{\circ}$ C and an upper ocean heat content anomaly (measured by three ARGOS floats) that
44 extended to ~ 45 m water depth (Trenberth et al., 2018). Harvey crossed the edge of the Texas
45 shelf in the northwestern Gulf at 18.00 U.S. Central Time having intensified to category 3, and
46 reached category 4 strength by midnight of August 25 with sustained wind speeds of 60 m/s (115
47 kt) and a minimum central pressure of 937 mbar (Blake and Zelinsky 2018). Rapid
48 intensification of tropical cyclones over the shallow waters of the south Texas shelf has been
49 reported previously and is believed to be related to periods when warm water occupies the whole
50 water column. This prevents mixing of colder bottom water that can reduce the energy flux
51 feeding the hurricane (Potter et al., 2019). The storm came ashore near Corpus Christi, TX on 26
52 August, and stalled over the TX coast, moving slowly to the northeast until August 31, after
53 which it moved inland and dissipated over Kentucky (Fig. 1).

54
55 Harvey brought a storm surge of up to 3 m and torrential rain to the Texas coast, with more than
56 1200 mm (48 in) of rain being recorded at 18 stations during its passage. The heaviest rainfall
57 was measured in Harris County, TX, at Nederland and Groves, near Houston, where over 1500
58 mm (60 in) fell (Blake and Zelinsky, 2018). Heavy rain (<500 mm) also affected Louisiana
59 (Fig.1). This unprecedented rainfall, the highest ever recorded in the U.S. for a tropical cyclone,
60 resulted in widespread flooding in Texas and Louisiana, more than 80 fatalities, and over \$150



Fig.1



61
62 Fig. 1. Track of Hurricane Harvey and associated rainfall over the southern United States, August 24-September 4,
63 2017 (from Blake and Zelinsky, 2018). The numbers 1 and 2 denote the positions of Galveston Bay and Matagorda
64 Bay respectively.

65
66 billion in economic damage (Emanuel, 2017; Balaguru et al., 2018). It is estimated that the total
67 amount of water that fell as rain over Texas and Louisiana during Harvey's passage was between
68 $92.7 \times 10^9 \text{ m}^3$ (Fritz and Samenow, 2017), and $133 \times 10^9 \text{ m}^3$ (DiMarco, unpublished), and over
69 200 mm of rain was recorded as far inland as Tennessee and Kentucky as the storm died down
70 (Blake and Zelinski, 2018; Fig.1). In addition to the rain that fell on land, DiMarco (unpublished)
71 has estimated that about another $44 \times 10^9 \text{ m}^3$ fell over the ocean.

72
73 Galveston Bay collects the runoff from the Houston metropolitan region. Following the storm,
74 the bay became a freshwater lake (Du et al., 2019; Steichen et al., 2020; Thyng et al., 2020) as it
75 was flushed with about three to five times its volume of rainwater. U.S. Geological Survey
76 (USGS) data (downloaded from <https://waterdata.usgs.gov>) show very rapid increases in flow
77 rates in Texas rivers and streams following the storm's landfall. For instance, flows in the
78 Colorado and Brazos Rivers (USGS stations 08162000 and 08111500 respectively; Figs S1a and
79 S1b) increased from $<2,000 \text{ cfs}$ ($\sim 60 \text{ m}^3/\text{s}$) during most of August to over $90,000 \text{ cfs}$ ($>2,500$
80 m^3/s) by the beginning of September, while flow in both the San Jacinto River (USGS station



81 08068090, Fig. S1c) and the Trinity River at Liberty (USGS station 08067000, Fig. S1d)
82 exceeded 100,000 cfs ($\sim 3,400 \text{ m}^3/\text{s}$). Flow in the Trinity River, which is generally the major
83 source of fresh water to Galveston Bay, increased from 20,800 cfs ($\sim 600 \text{ m}^3/\text{s}$) on August 27 to
84 100,000 cfs ($\sim 3,400 \text{ m}^3/\text{s}$) on August 31. The gauge at this site was unfortunately not in
85 operation immediately prior to August 27 or after September 9, but during June flowrates were
86 typically 10,000 – 14,000 cfs ($\sim 300\text{-}420 \text{ m}^3/\text{s}$). Such large changes in runoff are known to
87 produce major changes in estuaries and coastal waters (e.g., Ahn et al., 2005; Paerl et al., 2001,
88 2006; Mallin and Corbett, 2006; De Carlo et al., 2007; Zhang et al., 2009; Du et al., 2019; Thyng
89 et al., 2020). Runoff can add nutrients, heavy metals, oil and other organics, soil, and debris, all
90 of which can affect the local biota either positively (e.g., increasing local productivity through
91 nutrient input) or negatively (e.g., through salinity reduction, toxicity, smothering or reducing
92 biomass through eutrophication). Liu et al. (2019) and Steichen et al. (2020) reported changes in
93 the phytoplankton community within Galveston Bay as the salinity decreased and then increased
94 again.

95

96 Given the amount of rainwater released during the passage of the hurricane, it is not surprising
97 that there was massive runoff, including turbidity plumes that were visible well offshore (Fig.
98 S2). D'Sa et al. (2018) monitored large increases in terrestrial carbon ($25.22 \times 10^6 \text{ kg}$) and
99 suspended sediments ($314.7 \times 10^6 \text{ kg}$) entering Galveston Bay during the period 26 August-4
100 September. The plume off Galveston Bay on 31 August extended at least 55 km offshore (Du et
101 al., 2019), and surface water with a salinity of 15 was measured on 1 September at the Texas
102 Automated Buoy System (TABS) buoy F (28.84°N , 94.24°W ; yellow diamond in Fig. S2),
103 where it is typically 31-32 (data from <https://tabs.gerg.tamu.edu>). Normal salinities did not return
104 until 8 September. Similar sediment plumes at the mouths of the Brazos and Guadalupe estuaries
105 can be seen in Fig. S2, and such plumes and lowered salinities have been reported from the
106 Lavaca-Colorado and Nueces-Corpus estuaries near Corpus Christi (Walker et al., 2021). It is
107 likely that other bays and estuaries along the Texas coast were similarly affected, as they were all
108 under the path of the hurricane.

109

110 We report here on data collected before and after the hurricane along the Texas coast between
111 Galveston and Padre Island, Texas. Two cruises were completed prior to the advent of Hurricane



112 Harvey as part of a separate project. Following the hurricane, we completed three more cruises,
113 occupying the same stations in September (twice) and November 2017. This paper reports on the
114 changes in the water column between the pre- and post-hurricane cruises as they relate to
115 stratification, nutrient supply and oxygen concentrations.

116

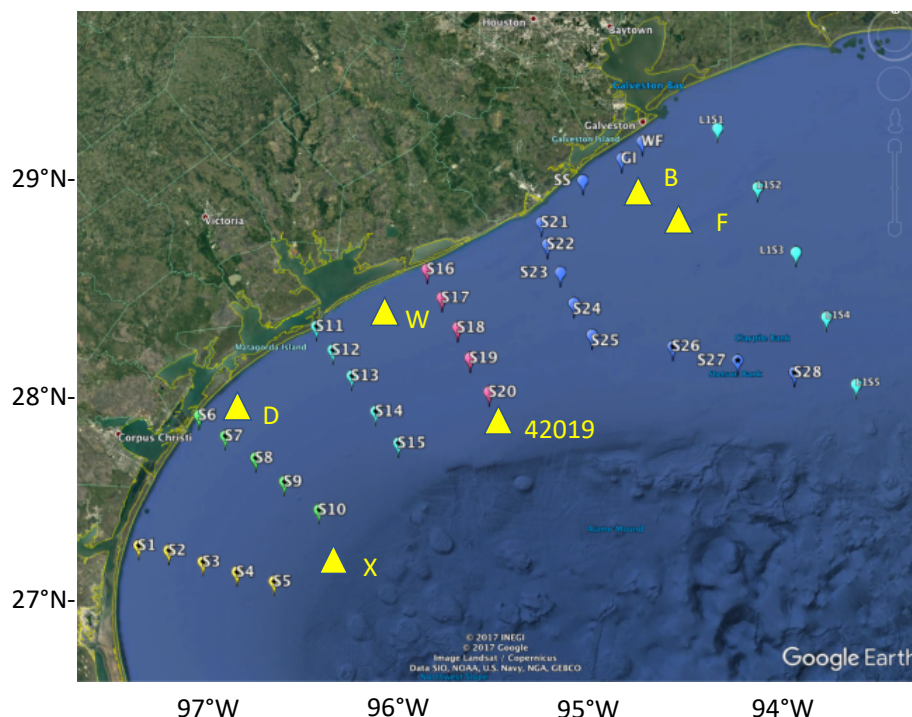
117 **2. Methods**

118 Pre-hurricane cruises on the R.V. *Manta* took place in June (12-16) and August (7-11) 2017,
119 while post-hurricane cruises were from 22-27 September, 29 September – 1 October, and 15-20
120 November on the R.V. *Point Sur*. The 27 September-1 October cruise only occupied the two
121 inshore stations on each line; all other cruises covered a standard grid of five lines of five
122 stations each (Fig. 2), together with supplemental *ad hoc* stations between lines and offshore in
123 the east of the region towards the Flower Gardens Banks National Marine Sanctuary, a shallow
124 reef system 120 km south of Galveston Bay near 27.92°N, 93.75°W. During the November
125 cruise, additional stations were added at the outer ends of the southernmost lines to ensure
126 sampling of Gulf of Mexico offshore surface water with salinity >35. Depths at the outer ends of
127 each line decreased from 95-110 m at stations 5 and 10 to 85 m at station 15, and 50 m at stations
128 20 and 25.

129

130 At each station, a full-depth CTD cast was made using a SeaBird 911 CTD fitted with a SBE-55
131 temperature sensor, SBE-3 conductivity sensor, SBE-45 pressure sensor, and a SBE-43 oxygen
132 probe. Additional sensors on the rosette package included a Chelsea Instruments Aqua3
133 fluorometer and a Biosperical/Licor PAR sensor. Discrete samples were collected from a 6-
134 bottle rosette for salinity determinations ashore and for oxygen calibration by Winkler titration
135 on board ship. Nutrient samples were collected, filtered, frozen on board and analyzed ashore for
136 nitrate, nitrite, phosphate, silicate, and ammonia by standard autoanalyzer methods (WHPO
137 1994). Limits of detection are about 0.1 $\mu\text{mol/L}$ for nitrate, silicate and ammonia, and 0.02
138 $\mu\text{mol/L}$ for nitrite and phosphate. Local meteorological data were collected by the ship's system,
139 while surface water temperature and salinity data came from the ships' flow-through system.

140



141
142 Fig. 2. Stations occupied during the four cruises. Only stations S1-S25 and the inshore stations GI, SS and WF were
143 occupied during June and August. All stations shown were occupied in September (22-27) and November. Only the
144 two inshore stations on each line were occupied during the second September cruise. Yellow triangles show
145 positions of TABS moorings B, D, F, and W, and NOAA buoy 42019.
146

147 Wind and current data are available from the TABS moorings along the Texas coast (see Fig. 2
148 for positions and <http://tabs.gerg.tamu.edu> for the data archive). Buoy B (off Galveston)
149 provided both wind and current data from before Harvey's landfall with a gap in the first half of
150 August); buoys W (off Matagorda Bay) and D (off Corpus Christi) provided current data only.
151 We have used additional wind data from TABS buoy X, which provided data until it failed on
152 the morning of 25 September, and NOAA buoy 42019 (29.91°N, 95.34°W, obtained from the
153 National Data Buoy Center at <https://www.ndbc.noaa.gov>).

154
155 Fluorometer data were obtained at each station sampled using a Chelsea Aqua 3 instrument on
156 the rosette. Satellite imagery (Level 2 Ocean Color files) obtained by the Aqua-1 MODIS sensor
157 downloaded from the NASA Goddard ocean color website (<https://oceancolor.gsfc.nasa.gov>)



158 were processed using the NASA SeaDAS software. In reality, the satellite-derived values may be
159 too high, due to the presence of CDOM after the storm (D'Sa et al., 2018), as the OC3 algorithm
160 provided by the SeaDAS software cannot discriminate between chlorophyll *a* and CDOM.

161

162 **3. Results**

163 **3.1 Wind fields**

164 Wind data from all moorings (not shown) were typical of summer conditions in this part of the
165 Gulf of Mexico, being predominantly from the south with occasional reversals (Nowlin et al.,
166 1998). At TABS buoy B, wind velocities during June and July were generally 5-8 m/s and varied
167 between SSE and SSW. Following a gap in data from 31 July until 22 August, they remained in
168 this quadrant until the passage of the hurricane, although wind speeds increased from 3-4 m/s on
169 August 22 to 12 m/s on August 29 when they were from the north. Following the passage of the
170 hurricane, winds again were predominantly from the SE/SSE during September, with the
171 exception of two short-lived reversals on September 5 and 10-12. Wind speeds during these
172 reversals were around 4-7 m/s.

173

174 Further south and offshore, at TABS mooring X and NOAA mooring 42019, weak northerly
175 winds (generally <4 m/s) were experienced from 6-8 June, with a second northerly spell from 20-
176 22 June, when speeds reached 10 m/s and mooring X and 15 m/s at 42019. After this second
177 frontal system moved through, winds reverted to SE/SSE at both moorings until the passage of
178 Hurricane Harvey at the end of August. During September, at mooring 42019, winds were
179 primarily from the NNE/ENE at 4-10 m/s until the 12th, and again from the 27th, with SE or
180 easterly winds of 3-7 m/s from September 14-26. Maximum sustained wind speeds recorded
181 during the hurricane at this mooring were 17 m/s, with gusts to 22.6 m/s. During October, there
182 were two northerly/westerly wind events, on the 16th, when winds reached speeds of 15m/s, and a
183 sustained event from 25-28 October, again with speeds <15 m/s. Northerly winds continued
184 during November, with sustained winds of 12-14 m/s during the periods 8-11, 18-20, and 22-24.

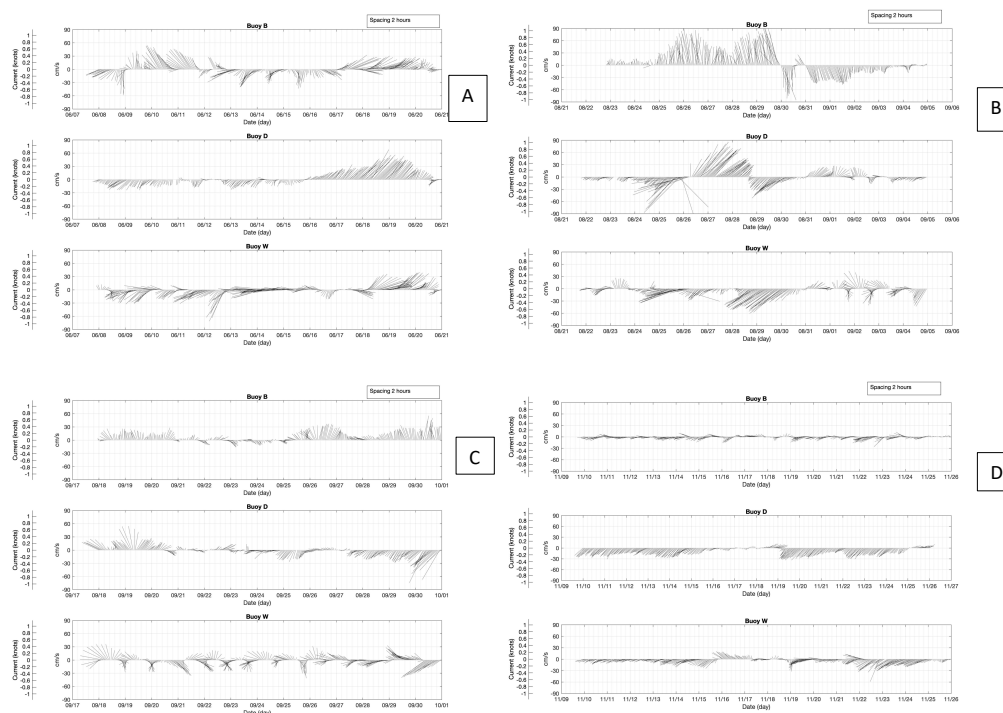
185

186 **3.2 Water movement**

187 Water movement over the Texas shelf is typically downcoast (towards the southwest) in non-
188 summer months and upcoast (towards the northeast) in summer, with currents following the wind



189 (Cochrane and Kelly, 1986; Walker, 2005). Upcoast winds and currents promote upwelling and
 190 act to retain water from the Mississippi-Atchafalaya system on the east Texas-Louisiana shelf
 191 (Hetland and DiMarco, 2008), while downcoast flow is downwelling-favorable and can reduce
 192 local stratification. During June 2017, currents at Buoy D (27.96° N, 96.84° W) were essentially
 193 downcoast from prior to the cruise until June 15, when they switched to upcoast until June 20,
 194 after which they flowed downcoast again (Fig. 3a). The current reversal took place slightly later
 195 (June 17) at Buoys B (28.98° N, 94.90° W) and W (28.35° N, 96.02° W), but the return to
 196 downcoast flow again occurred on 20 June at both sites (Fig. 3a). These three moorings are all
 197 situated close to the coast in water depths of 20 +/- 2 m.
 198



199
 200 Fig. 3. Current vectors at TABS buoys B, D and W during (A) the June cruise, (B) the period of the hurricane
 201 (August), and the cruises in September (C) and November (D).

202
 203 Upcoast currents prevailed at sites W and D during the August cruise (Fig. 3), although currents
 204 were downcoast from about August 8-10 at W and 9-11 at site D (not shown). Buoy B did not



205 record current speeds during this period, but was back in service immediately before the
206 hurricane arrived. During the passage of the hurricane, the southernmost mooring (buoy D)
207 recorded strong currents of > 1 m/s which changed from downcoast to upcoast and back to
208 downcoast again as the storm moved towards the northeast (Fig. 3b). Buoy W recorded
209 continuous downcoast currents during the period of the hurricane, while buoy B showed strong
210 onshore currents (< 1.0 m/s) until August 30, when currents reversed to offshore at < 80 cm/s.
211 Following the hurricane, coastal currents were considerably weaker at all three sites in
212 September and November. During the September cruise there were a number of current
213 reversals, especially at buoy W, although velocities were generally < 30 cm/s (Fig. 3c). By
214 November, current velocities decreased still further and the expected flow towards the west was
215 reinstated (Fig. 3d).

216

217 **3.3 Temperature, precipitation and salinity**

218 Temperatures measured during the cruises (not shown) showed well-mixed or weakly stratified
219 water inshore in June and August with surface-bottom differences of less than 2° at the two
220 inshore stations on each line. Further offshore, bottom temperatures decreased with depth but
221 there remained a well-mixed surface layer of 15-25m thickness. Following the hurricane,
222 however, the mixed layer extended further offshore, including the third station along each line in
223 September and almost all stations in November, when isothermal water was found as deep as
224 80m in some instances, and bottom temperatures were often warmer than at the surface.

225

226 Surface temperatures across the region increased from about 28.5°C during the June cruise to
227 over 30°C in August (Trenberth et al., 2018). As the hurricane passed through the region,
228 temperatures measured at the buoys, including at NBDC buoy 42019 (27.91°N , 95.34°W),
229 decreased to a minimum of about 27.5°C , but recovered to 28.5 - 29°C by the time of the
230 September cruises. By November, temperatures had decreased to 21 - 22°C , 22 - 23°C and 23 -
231 23.5°C at buoys B, W and D respectively. NBDC buoy 42019, which is further offshore than the
232 TABS moorings in 82 m of water, registered temperatures of between 25.4 and 26.0°C during
233 this period.

234



235 Table 1. Precipitation rates (cm) for sites in central Texas from May-September 2017 compared with the long-term
 236 mean (*italics*). Data downloaded from https://www.srcc.tamu.edu/climate_data_portal/?product=precip_summary
 237 (accessed 7.07.2021).

	May	June	July	Aug	Sept
239 Austin International airport	7.59	6.17	2.69	32.99	9.68
241	<i>11.86</i>	<i>8.28</i>	<i>4.65</i>	<i>6.20</i>	<i>8.46</i>
242					
243 Corpus Christi airport	8.18	4.90	3.22	14.98	3.71
244	<i>8.51</i>	<i>8.00</i>	<i>5.97</i>	<i>7.87</i>	<i>13.41</i>
245					
246 Houston Hobby airport	6.81	13.20	7.92	98.73	9.52
247	<i>12.80</i>	<i>13.84</i>	<i>11.40</i>	<i>11.81</i>	<i>13.13</i>
248					
249 Houston Intercontinental airport	6.12	18.26	15.98	99.34	3.12
250	<i>13.59</i>	<i>14.22</i>	<i>9.45</i>	<i>11.10</i>	<i>12.09</i>
251					
252 San Antonio airport	4.48	1.02	0.41	14.91	7.11
253	<i>10.18</i>	<i>8.58</i>	<i>5.92</i>	<i>6.12</i>	<i>9.32</i>
254					
255 Victoria	7.77	8.92	0.94	43.03	7.92
256	<i>12.85</i>	<i>11.10</i>	<i>8.25</i>	<i>7.82</i>	<i>12.52</i>

257

258 Precipitation rates for a number of stations in central Texas are shown in Table 1. With the
 259 exception of the August data, all stations reported lower than average rainfall during these
 260 months apart from Houston Intercontinental Airport in June and July, and Austin International
 261 Airport in September (respectively north and northwest of Galveston Bay). Despite this, low
 262 salinities were found in June at the surface inshore and pushing southwards (Fig. 4a), with a
 263 strong, sloping salinity front between the surface layer and the deeper water. Salinity values
 264 across the front changed by ~12 psu along stations 18-20 and 21-23 just south of Galveston Bay.
 265 The salinity gradient decreased towards the south, with an inshore-offshore change of only 4 psu
 266 south of 28°N. The lowest surface salinity (station 21) was <22 at this time, and was still <32
 267 along the southernmost line except at the outermost station. Bottom water salinities (not shown)
 268 were higher because of density stratification, with salinities of >35 found in water deeper than
 269 about 20m at stations in the eastern half of the grid and 35 m on the southern lines. The low
 270 surface salinities were most likely caused by westward flow from the Mississippi-Atchafalaya
 271 river system (MARS), together with local outflow from Galveston Bay. The MARS peaked

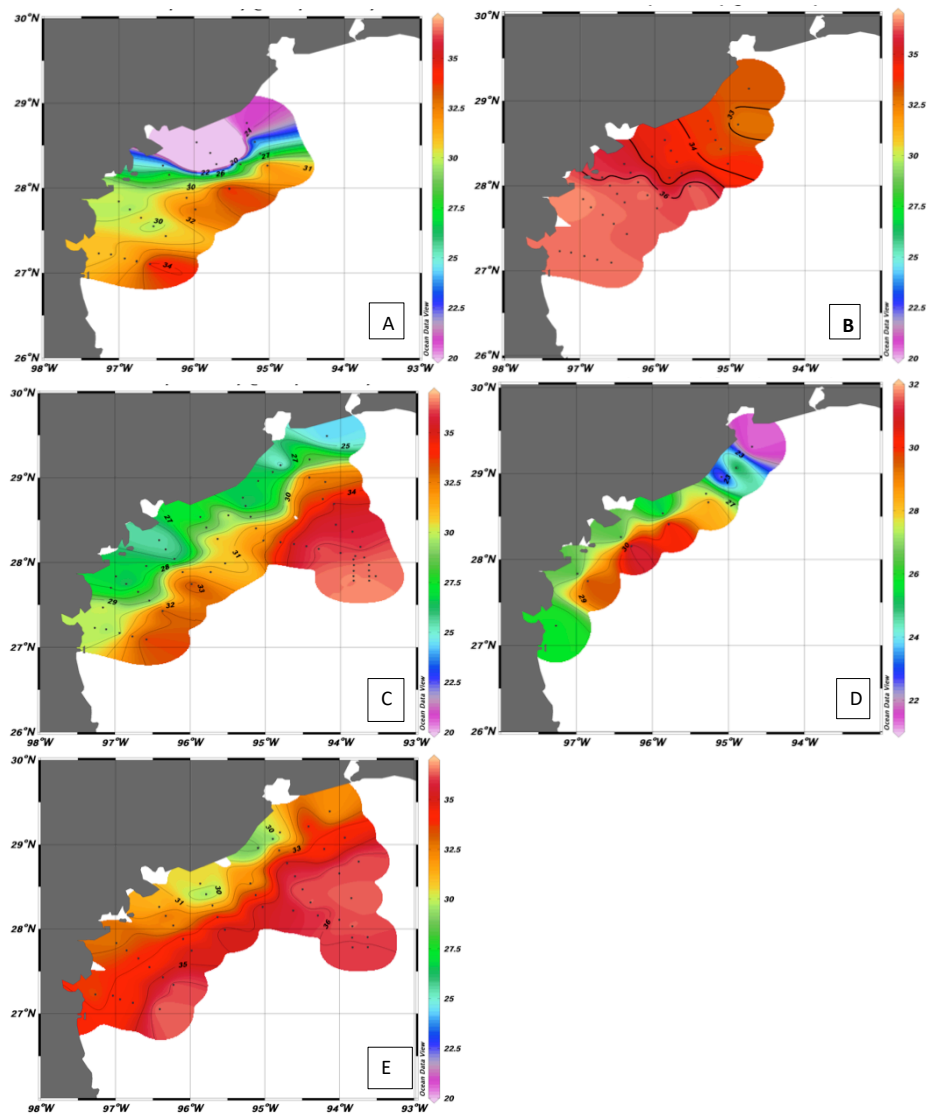


Fig. 4. Surface salinities during 2017 cruises in (a) June, (b) August, (c) September 22-27, (d) September 29 – October 1, and (e) November.

272

273 during the 2017 spring flood at 1.22 Mcfs (34,500 m³/s), almost double the long-term mean from

274 1935-2017 (data from <http://rivergages.mvr.usace.army.mil/>, accessed 7.07.2021).



275

276 By August (Fig. 4b), surface salinities had increased across the region as a result of the southerly
277 winds, with a minimum of 32.15 just south of Galveston Bay, while the 35 surface isohaline was
278 situated off Matagorda Bay between stations 16-20 and stations 11-15. Bottom water was still
279 stratified at stations on the two northern lines, with salinities <35 only found at stations 16, 17,
280 21, and 22 and at the Wind Farm (29.14° N, 94.75° W). Further south, stations 1-10 and 13-15
281 all contained almost isohaline water with $S > 36$.

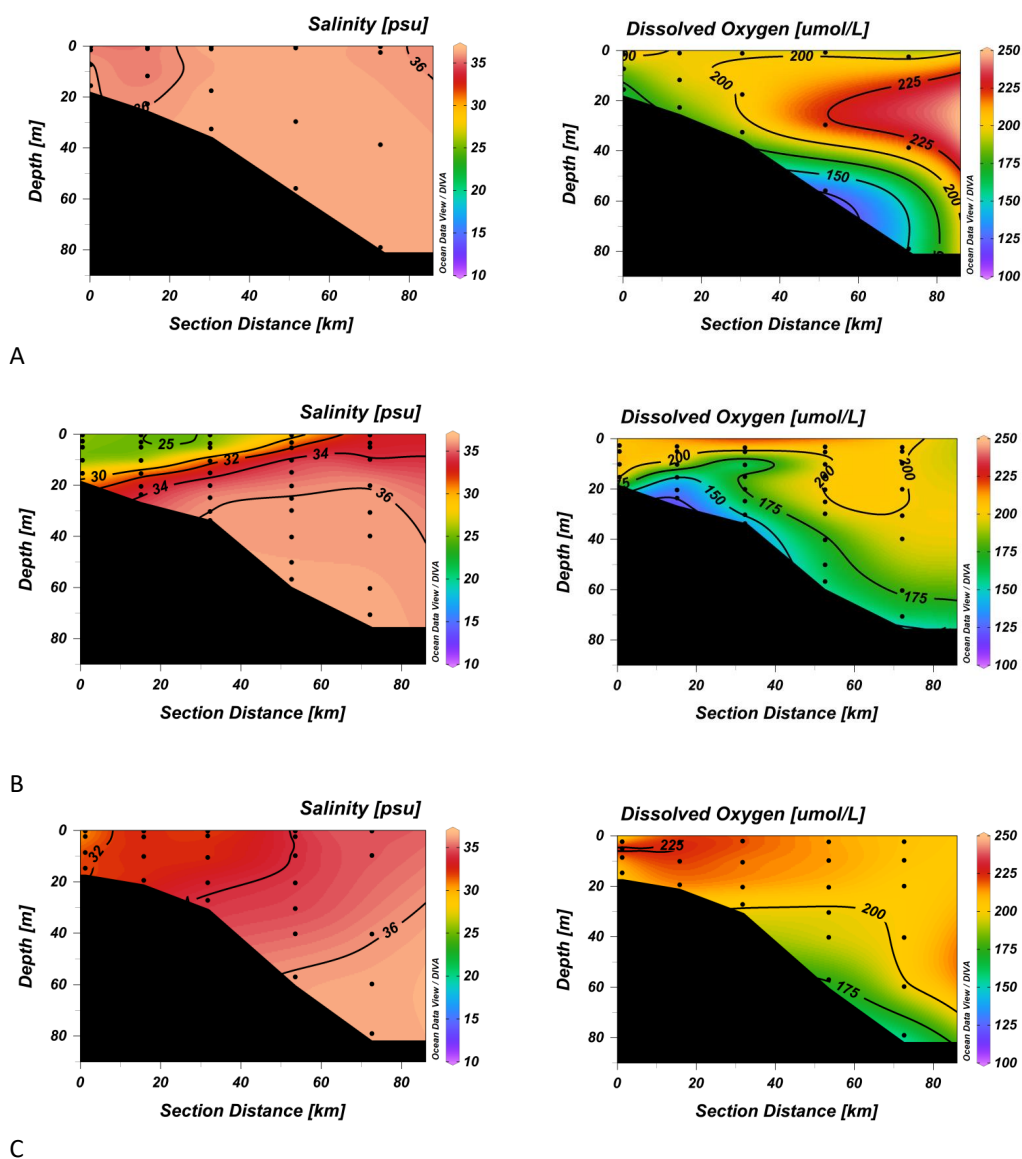
282

283 The fresh water from the hurricane caused a major change in the surface salinity by the time of
284 the first September cruise (22-27), resulting once again in a strong cross-shelf gradient (Fig. 4c).
285 Surface salinities were <33 throughout the region, apart from two stations at the extreme south of
286 the grid, where it was just above 33, and in the area more than 100 km offshore between
287 Galveston Bay and the Flower Gardens Banks, where there was a strong salinity front. A similar
288 situation was found a week later at the inshore stations (Fig. 4d), although the surface layer of
289 low salinity water had thinned and was confined to the innermost stations on each line. Vertical
290 sections in September showed very strong stratification of up to 10 psu within a 10-m depth
291 interval along all lines (e.g., Fig. 5; this section across stations 11-15, adjacent to Matagorda
292 Bay, is taken as representative for all five lines). The halocline was not flat, but deepened
293 towards the coast, giving a wedge of lower salinity water onshore, and the depth at which it
294 intersected the bottom decreased from ~30m in the north to less than 20m in the south. Water
295 with salinity > 36 was found at the bottom on all lines. By November (Figs 4e, 5), however, a
296 more typical salinity field was found, with well-mixed water throughout the coastal zone and a
297 general onshore-offshore gradient at all depths. This is normal for the region in the fall, when
298 atmospheric frontal systems tend to move across the Texas shelf and break down the summer
299 pycnocline (Cochrane and Kelly, 1986; Nowlin et al., 1998).

300

301 **3.4 Oxygen concentrations**

302 Oxygen concentrations in this region of the Gulf of Mexico are typically saturated above the
303 pycnocline, and this was the case during all four cruises, with concentrations between 210-220
304 $\mu\text{mol/L}$ in June (not shown), when the surface temperature was around 25° C, and 190-215
305 $\mu\text{mol/L}$ during August and September, when it was nearer 30° C (Fig. 5). By November, with



306
307 Fig. 5. Salinity (psu) and oxygen ($\mu\text{mol/L}$) sections across line 3 (stations 11-15) for the August (a), September (b)
308 and November (c) cruises.

309

310 declining surface temperatures, the saturation concentration increased to between 210-230
311 $\mu\text{mol/L}$. Below the pycnocline, oxygen concentrations declined in the higher salinity water. This
312 effect was most pronounced offshore in June and August, when subtropical underwater, with



313 typical oxygen concentrations of 160-170 $\mu\text{mol/L}$, intruded onto the outer shelf (Fig. 5). Isolated
314 patches with concentrations $<150 \mu\text{mol/L}$ were seen over the mid-shelf and across the eastern
315 part of the grid at this time. This situation had changed considerably by the time of the
316 September cruises, with bottom concentrations of 150 $\mu\text{mol/L}$ or less over large parts of the
317 inner and middle shelf and at the outermost stations of the grid. Vertical sections showed that the
318 lowest oxygen concentrations occurred at the base of the pycnocline where it intersected the
319 seafloor (Fig. 5), but hypoxia (oxygen concentrations $<62 \mu\text{mol/L}$) was not observed at any
320 station. There was little change in either the pattern of oxygen distribution or concentrations at
321 the innermost stations between the two cruises in September (not shown). By November,
322 however, after the passage of a number of frontal systems with wind speeds up to 14 m/s, the
323 oxygen concentrations showed little vertical structure and the system could be said to have
324 returned to normal for that month.

325

326 **3.5 Nutrients**

327 Nutrient concentrations in the coastal waters along the Texas coast in summer are typically very
328 low at the surface, increasing with depth even on the shallow shelf as nutrient regeneration takes
329 place near the bottom. This is especially the case when hypoxic events occur (Nowlin et al.,
330 1998; DiMarco and Zimmerle, 2017; Bianchi et al., 2010). Mean concentrations in the upper
331 30m of the water column for all nutrients at stations within the grid as well as at additional
332 stations having water depths shallower than 50m are given in Table 2. Data from the second
333 September cruise, which covered only the two inshore stations on each line, are not included in
334 the table. These data showed similar patterns to the cruise a week earlier, although mean
335 concentrations were higher because of the proximity of the coast and the many freshwater
336 discharges from bays and rivers.

337

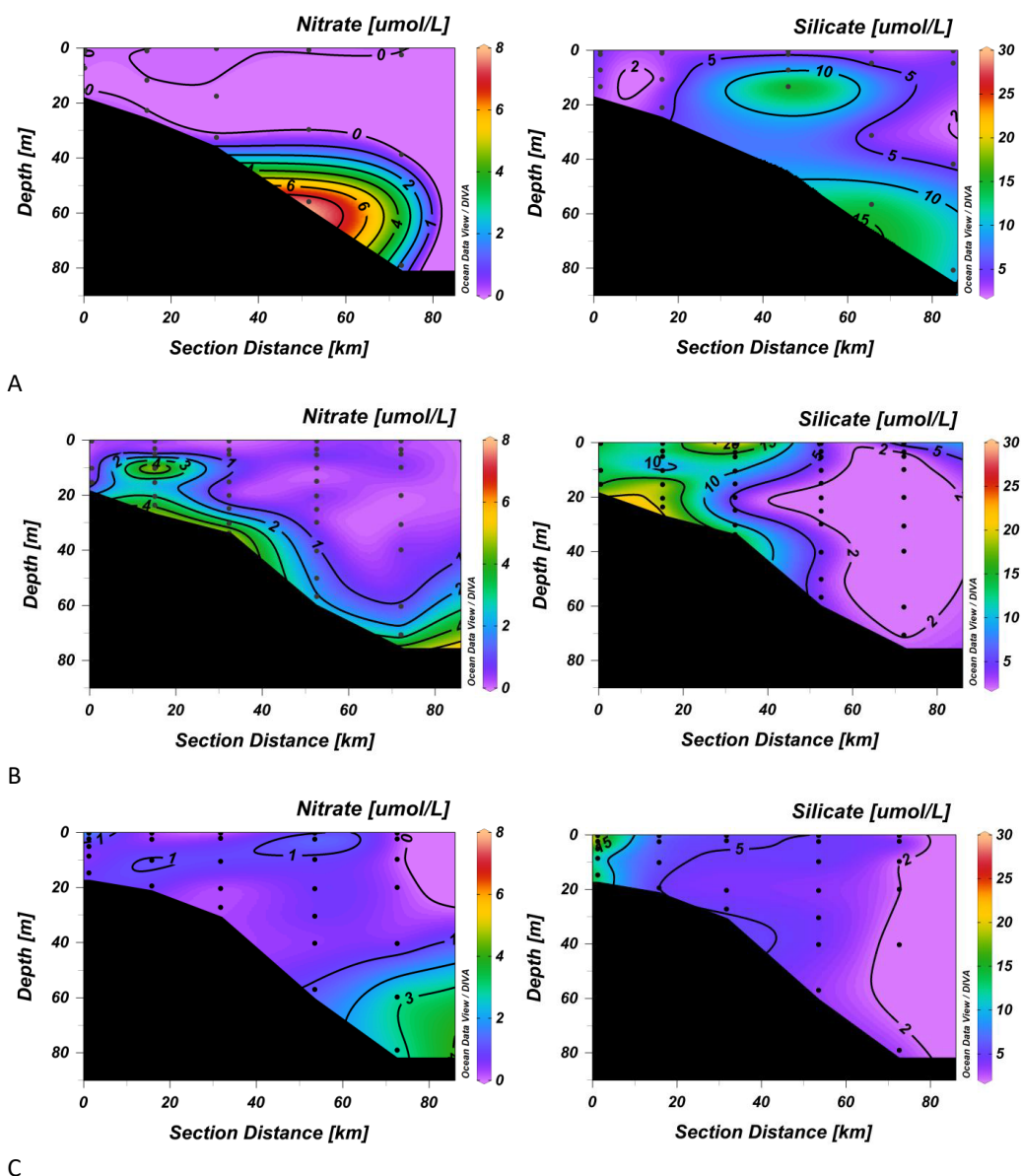
338 In higher salinity (>35) water and offshore, nutrient concentrations increase only slowly with
339 depth and nitrate and silicate concentrations $> 5 \mu\text{mol/L}$ are generally found in midwater only
340 below depths of about 50 and 100m respectively (Fig. 6, Supplemental Fig. S3). Only one nitrate
341 sample (in September) containing more than 8 $\mu\text{mol/L}$ came from below 60m depth. Nitrite
342 concentrations were almost all low, with mean concentrations in the upper 30m below 0.5
343 $\mu\text{mol/L}$ on all four cruises, although individual surface concentrations were considerably higher.



344 Table 2. Mean, range and number of samples (N) for nitrate, nitrite, ammonia, phosphate and silicate in the upper
 345 30m of the water column for all four cruises. DIN is calculated as the sum of the three nitrogen species. DIN:P and
 346 DIN:Si ratios use the values for all individual samples.
 347

		June	August	September	November
Nitrate	Mean	0.71	0.10	0.57	0.52
	Range	0.00-10.60	0.00-1.98	0.00-7.41	0.00-1.98
	N	85	94	194	164
Nitrite	Mean	0.43	0.18	0.44	0.36
	Range	0.00-2.80	0.00-1.04	0.03-4.76	0.00-1.13
	N	86	98	196	172
Phosphate	Mean	1.07	0.65	1.30	1.00
	Range	0.21-2.85	0.00-3.55	0.00-5.63	0.00-3.24
	N	85	91	190	169
Silicate	Mean	6.00	5.04	7.00	7.76
	Range	1.18-26.89	0.00-20.09	0.00-40.23	0.94-25.71
	N	84	89	193	168
Ammonia	Mean	1.90	3.74	2.39	2.91
	Range	0.00-7.62	1.37-8.05	0.08-4.97	0.89-4.80
	N	84	87	192	162
DIN	Mean	3.01	3.70	3.37	3.72
	Range	0.01-14.47	0.14-8.56	1.02-12.35	1.05-7.03
	N	85	95	191	160
DIN:P		3.56	11.95	4.98	10.11
	Range	0.03-25.86	0.00-324	0.00-138	0.00-381
DIN:Si		0.63	2.59	1.17	0.78
	Range	0.00-3.20	0.00-53.29	0.00-25.21	0.10-4.78

348 Ammonia concentrations were also variable, particularly inshore, and generally provided a
 349 background concentration of about 2-4 $\mu\text{mol/L}$. As a result, DIN distribution closely resembled
 350 that for nitrate but with the contribution from ammonia (Fig. S4).
 351



352

353 Fig. 6. Nitrate and silicate ($\mu\text{mol/L}$) sections along line 3 (stations 11-15) during August (a), September (b) and
354 November (c) cruises.

355

356 Phosphate concentrations (not shown) were similarly lower at the surface than at depth, except in
357 September, when the influence of surface runoff gave rise to concentrations above 3 $\mu\text{mol/L}$ in
358 the upper 10m of the water column and a background concentration between 1.5 – 3 $\mu\text{mol/L}$ in



359 the rest of the water column up to 50 km offshore (between stations 13 and 14). Phosphate is
360 almost always non-limiting for phytoplankton in this region, so that residual phosphate
361 concentrations can be found even though nitrate is depleted (Bianchi et al., 2010), although
362 Sylvan et al. (2006, 2007) and Quigg et al. (2011) have suggested phosphate limitation can occur
363 further east in the Mississippi plume. Silicate, however, showed an opposite trend to the general
364 pattern of the other elements, with almost all samples $>15 \mu\text{mol/L}$ coming from the upper 25m of
365 the water column, and concentrations decreased with depth to $<5 \mu\text{mol/L}$ below 100m (Figs 6,
366 S3). Silicate also showed a cross-shelf gradient, particularly along the two southernmost lines
367 (not shown).

368

369 This general distribution shown in Figs. 5 and 6 was seen during early summer along all the lines
370 occupied during June and August. In June, high concentrations of both nitrate and silicate were
371 seen at stations 21 and 22, immediately south of Galveston Bay, where bottom water oxygen
372 concentrations were $<90 \mu\text{M/L}$; elsewhere midwater levels of both elements were low, with very
373 low nitrate concentrations ($<0.5 \mu\text{mol/L}$) being found even at the bottom at some stations. While
374 silicate concentrations were more variable, highest concentrations were typically again seen at
375 the bottom, and midwater concentrations were generally $<5 \mu\text{mol/L}$. The situation was similar in
376 August (Fig. 6), when nitrate was very low throughout the region, and even bottom nitrate values
377 were below detection at many stations.

378

379 In September, despite the extreme freshwater runoff, nitrate concentrations were still low except
380 near the bottom at shallow stations, and there was little sign of any surface or mid-water increase
381 in concentration (Fig. 6). A comparison of nitrate concentration with depth gave essentially the
382 same distribution as during earlier cruises, although there were more samples within a depth
383 range of 10-30m showing concentrations above $2 \mu\text{mol/L}$ (Fig. S3). These samples came from
384 bottom samples at shallow stations where the oxygen concentration was reduced. The cross-shelf
385 gradient seen in silicate concentrations was more pronounced on this cruise, and concentrations
386 exceeded $10 \mu\text{mol/L}$ throughout the water column at all the inshore stations. However, by
387 November, concentrations of both nutrients had decreased considerably, although the offshore
388 silicate gradient was still present and concentrations $>10 \mu\text{mol/L}$ were found inshore (Fig. 6).



389 Phosphate concentrations higher than $2 \mu\text{mol/L}$ were seen only in September (Table 2),
390 suggesting the presence of terrestrial runoff following the hurricane.

391

392 Oxygen/nitrate and oxygen/silicate covariance plots are shown in Supplemental Fig. S5. High
393 nitrate values at oxygen concentrations greater than $200 \mu\text{mol/L}$ in August and September (22-
394 27) are from samples taken in low salinity surface water; where oxygen concentrations were
395 below $150 \mu\text{mol/L}$ the increase in nitrate concentration is caused either by regeneration over the
396 shelf or by the intrusion of deeper Subtropical Underwater. During these two cruises, higher
397 nitrate and silicate concentrations were associated generally with lower oxygen concentrations
398 (Fig. S5), although some surface samples on both cruises showed relatively high values,
399 associated with salinities < 35 .

400

401 Quigg et al. (2011) state that DIN concentrations $< 1 \mu\text{mol/L}$ and a DIN:P ratio < 10 indicate
402 nitrogen limitation, with $\text{P} < 0.2 \mu\text{mol/L}$ and $\text{DIN:P} > 30$ indicating P limitation and $\text{Si} < 2$
403 $\mu\text{mol/L}$, $\text{DIN:Si} > 1$ and $\text{Si:P} < 3$ showing Si limitation. As shown in Table 2, DIN:P and DIN:Si
404 ratios for individual samples in the upper 30m of the water column were low during all four
405 cruises, with mean DIN:P being less than the 16:1 Redfield ratio throughout, while the mean
406 DIN:Si ratio was > 1 only in the August and September cruises. This suggests both nitrogen
407 limitation throughout the period and possible silicate limitation of diatom growth during August
408 and September despite the background levels of ammonia that contributed to the DIN
409 concentration. While individual samples had higher ratios, these all occurred when either
410 phosphate or silicate concentrations were measurable but very low in comparison with DIN
411 concentrations ($< 0.1 \mu\text{mol/L}$ for P and $< 0.5 \mu\text{mol/L}$ for Si). The ratios of the mean
412 concentrations of DIN across the region to the mean concentrations of P and Si (e.g., 3.01:1.07
413 for DIN:P in June), were 2.81 and 0.50, 5.69 and 0.73, 2.59 and 0.48, and 3.72 and 0.48 for the
414 June, August, September and November cruises respectively, again suggesting nitrogen
415 limitation.

416

417 **4 Discussion**

418 One would normally expect that the amount of rainfall seen during Hurricane Harvey would
419 result in an exceptional flushing of nutrients into the coastal bays and the offshore coastal zone,



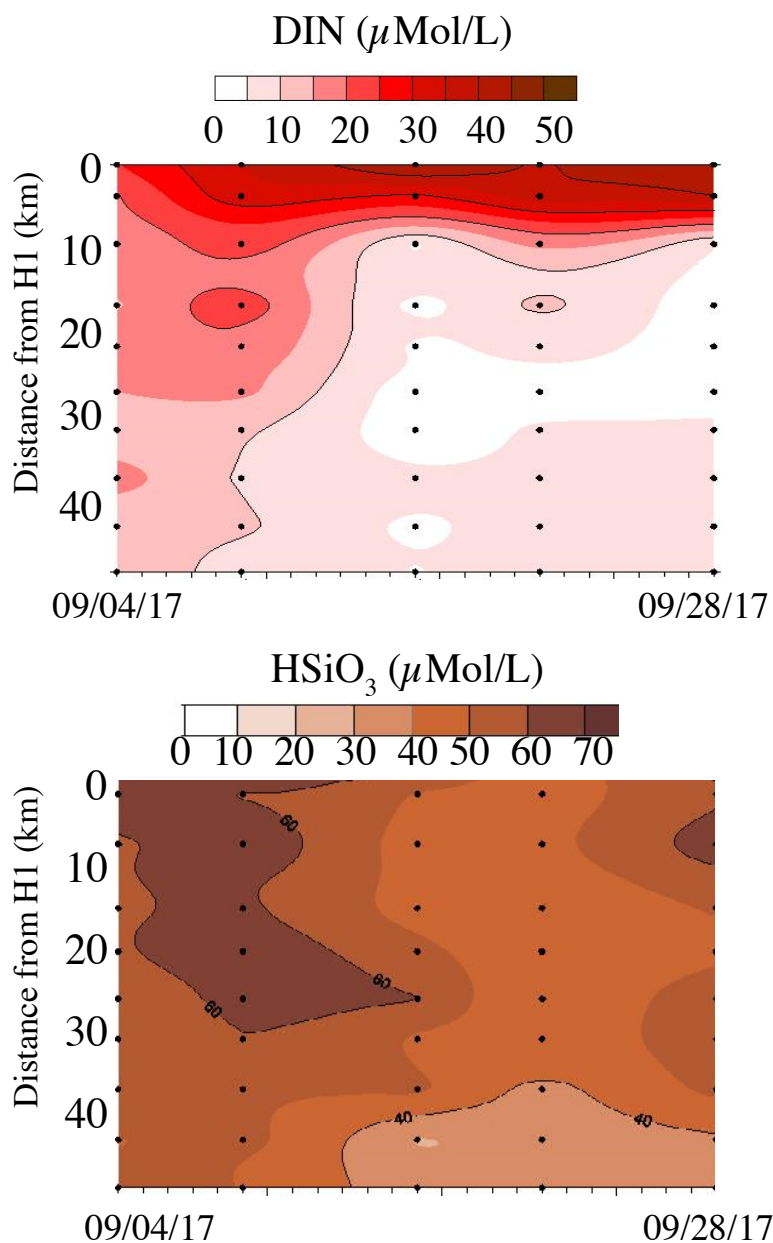
420 as found, for example, in Biscayne Bay, Florida, following Hurricane Katrina in 2005 (Zhang et
421 al., 2009), or in the Caribbean in 1998 following Hurricane Georges (Gilbes et al., 2001), leading
422 to short-lived phytoplankton blooms, but the data show very little sign of such a buildup
423 offshore, other than excess phosphate seen during the first September cruise (see above). The
424 coastal bays turned into freshwater lakes – Galveston Bay was flushed by about three to five
425 times its volume of freshwater (Du et al., 2019; Thyng et al. 2020) and this resulted in higher
426 concentrations of nutrients, particularly nitrate and silicate, as well as blooms of phytoplankton
427 and cyanobacteria within the bay (Liu et al., 2019; Steichen et al., 2020). DIN concentrations, in
428 particular, were greatly reduced two weeks after the hurricane had passed through the region and
429 were back to normal conditions by November (Steichen et al., 2020, Fig. 7; J. Fitzsimmons, pers.
430 comm.), with concentrations above $5 \mu\text{mol/L}$ only found in the uppermost parts of the system
431 after about 15 September. Silicate concentrations similarly dropped quickly within the first two
432 weeks, although they remained above $40 \mu\text{mol/L}$ throughout the bay during the sampling period.

433

434 Following hurricane Harvey, low-oxygen water containing $<160 \mu\text{mol/L}$ and nitrate
435 concentrations of $> 2 \mu\text{mol/L}$ penetrated further onto the shelf during September than during
436 either August or November (Figs. 5, S3). The high salinity of this water mass (>36 , Fig. 5)
437 suggests that it was Subtropical Underwater, which is found above 250 m in the northern Gulf
438 with typical core salinity of about 36.4 -36.5 near 100m depth in this region, and oxygen and
439 nitrate concentrations of about 110-150 $\mu\text{mol/L}$ and 6-15 $\mu\text{mol/L}$ respectively (Nowlin et al.,
440 1998). However, given the strong pycnocline shown by the salinity section (Fig. 5), there was
441 little opportunity for these additional nutrients to reach the surface layer and affect
442 phytoplankton production, and there is no evidence that such upwelling has resulted in hypoxia
443 in the past in this region.

444

445 Further south, the Matagorda-San Antonio-Aransas-Corpus Christi Bay system similarly showed
446 rapid short-term nutrient increases followed by hypoxia (Montagna et al., 2017; Walker et al.,
447 2021), but these were back to pre-storm concentrations by early October (Walker et al., 2021).
448 The levels in Guadeloupe Bay, an offshoot of San Antonio Bay, were followed at fortnightly
449 intervals from mid-August to mid-October and showed a rapid increase in nitrate but slower
450 increases in phosphate and silicate. This is not unexpected, given the solubility of nitrate ions



451

452 Fig. 7. Nitrate plus nitrite (a) and silicate (b) concentrations ($\mu\text{mol/L}$) measured along a transect through Galveston

453 Bay. Sampling dates were 9.04.17, 9.09.17, 9.16.17, 9.21.17, and 9.28.17. Station H1 was the innermost station in

454 the bay (see Steichen et al., 2020 for details).

455



456

457 relative to the other two. Thus, it appears that the increases in nutrient concentrations affected
458 mainly the coastal bays and estuaries rather than the offshore coastal zone. This backs up
459 conclusions of Sahl et al. (1993) following a cruise along the Louisiana-Texas shelf in March
460 1989 when river discharges were at their highest levels during that year. They found that
461 nutrients derived from bay systems dissipated within about 20 km of the bay mouths, and that
462 higher nutrient concentrations below 80 m depth resulted from upwelling along the shelf edge, in
463 agreement with the work of Chen et al. (2003) and Walker et al. (2005). Similar retention of
464 nutrients, leading to short-lived (2-3 weeks) phytoplankton blooms, has been reported following
465 hurricanes in the Neuse River/Pamlico Sound system in N. Carolina (Paerl et al., 2001, 2018;
466 Peierls et al., 2003), in Chesapeake Bay (Roman et al., 2005), and Biscayne Bay (Zhang et al.,
467 2009).

468

469 Although nutrient fluxes were undoubtedly greatly increased immediately following the
470 hurricane, nutrient concentrations in Texas rivers are only sampled infrequently, and data do not
471 exist to allow us to calculate the overall fluxes during this period. However, the available data
472 suggest that absolute concentrations did not change very much following the hurricane in most
473 instances (Table 3). The infrequent sampling by federal and state authorities, coupled with the
474 rapid decrease in river flow by about September 7 (Fig. S1), suggest that nutrient concentrations
475 in the coastal bays and the coastal ocean were likely diluted by the time of our survey in late
476 September. Du et al. (2019) point out that while the salinity at the mouth of Galveston Bay was
477 back to normal about two weeks after the storm, it took almost two months to recover at stations
478 further inside the bay and the same time period at offshore buoys. Similar effects are likely at
479 other bay sites along the Texas coast.

480

481 Changes in salinity during and following the storms were recorded at offshore moorings. During
482 the period around the passage of the hurricane, the TABS moorings showed rapid decreases in
483 salinity with a slow increase thereafter (data not shown). Buoy X (offshore) showed the least
484 variability, with salinities remaining near 36.4 until 9.04.17, dropping briefly to 35.3, but
485 recovering to above 36 again by 9.06.17. Buoy D, inshore near Corpus Christi, also recorded



486 Table 3. Nutrient concentrations in Texas rivers around the time of the hurricane ($\mu\text{M/L}$). Data taken from USGS
 487 and the Texas Commission on Environmental Quality (TCEQ) Clean Rivers Program for individual river basins.

488

489 a. Trinity River (Baytown; USGS site 08067525)

490 Date	Nitrate	Phosphate	Silicate
491 7.06.17	10.15	2.03	74.2
492 7.19.17	11.28	2.52	90.0
493 8.15.17	11.43	3.16	155.5
494 9.05.19	10.64	1.74	96.0
495 11.08.17	5.43	1.58	143.5

496

497 b. Trinity River (Liberty, USGS site 08067000)

498 8.16.17	<2.86	2.38	137.5
499 8.31.16	8.71	1.32	97.8
500 9.05.16	15.85	2.26	127.0

501

502 c. Brazos River (US 290; TCEQ site 11850)

503 7.26.17	41.40	<1.29	
504 8.22.17	7.86	<1.29	
505 9.27.17	12.86	2.26	
506 10.25.17	37.86	2.90	

507

508 d. Colorado River (La Grange; TCEQ site 12292)

509 6.06.17	2.86	92.58	
510 8.08.17	2.86	118.06	
511 10.02.17	2.14	86.45	

512

513 e. San Antonio River (Goliad; TCEQ site 12791)

514 7.19.17	<3.57		
515 9.06.17	<3.57		
516 11.01.17	<3.57		

517

518 salinities of about 36.6 until 8.23.17, dropping to 34.7 on 8.26, but were >36 a day later.

519 Salinities dropped again on 8.29, remaining in the range 32-34 until 9.06, after which they

520 dropped again to below 30, where they remained until 10.24.17, with a minimum salinity of

521 20.51 on 9.13. Further up the coast buoys B and F both experienced decreased salinities (buoy W

522 did not record salinities during the passage of the hurricane). Before the hurricane, salinities in

523 this region were in the range 32.5-34.5, with the higher salinities offshore. Following the passage

524 of the storm, buoy F recorded a minimum salinity of 15.25 on 9.01.17 and salinities <20 until

525 9.06.17. A salinity of 30 was only recorded again here on 9.08.17. The inshore buoy B recorded

526 minimum salinities in the range 19-21 on 8.30. These remained <23 until 9.09, and below 30 for



527 the remainder of the month, after which they increased again to around 32. The fact that the
528 minimum salinity was recorded at the offshore mooring is presumably related to the strength of
529 the plume emanating from Galveston Bay with enough momentum to overcome the Coriolis
530 force that would tend to push it to the southwest close to the coast (Du et al., 2019).

531

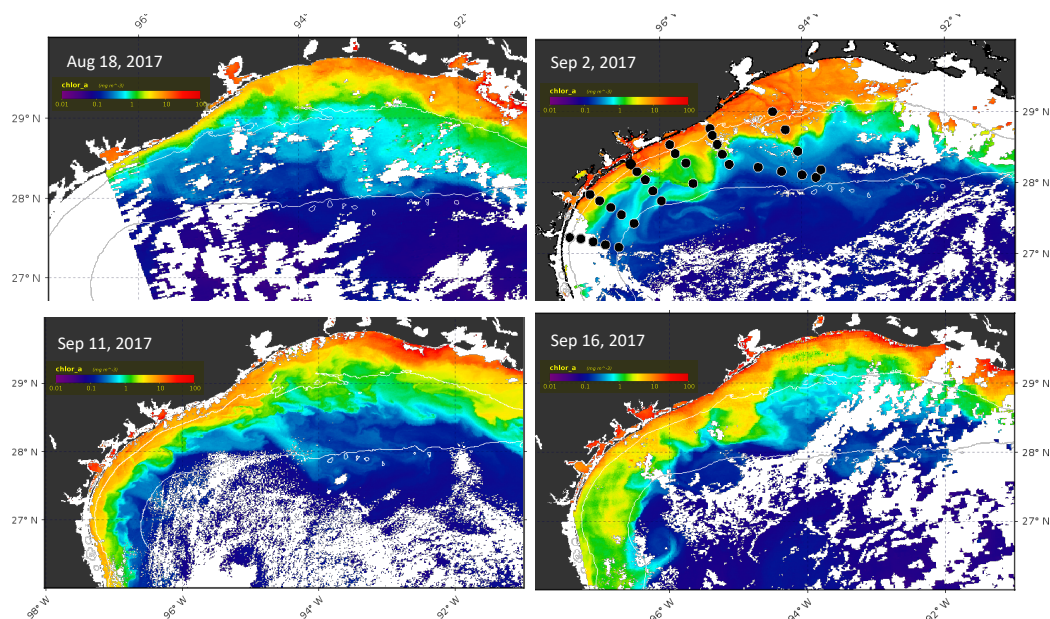
532 These data suggest that there was a slow southward movement of low salinity water along the
533 coast (see Figs. 4c, d) after the hurricane as the coastal current was re-established. The fact that
534 winds were from the east for almost the whole of September would have assisted this downcoast
535 movement, as described by Cochrane and Kelly (1986). Mixing during the infrequent northerly
536 wind bursts would cause salinities to increase again, although even in November salinities below
537 30 were still seen between Galveston Bay and Matagorda-Corpus Christi Bays (Fig. 4e).

538

539 The effects of the hurricane on phytoplankton productivity, as measured by chlorophyll
540 concentrations along the Texas shelf and slope, were examined using both in situ fluorescence
541 data obtained during the cruises and satellite imagery from the MODIS sensor on the Aqua
542 satellite (Fig. 8). The Texas coast and northwestern Gulf of Mexico were covered with clouds
543 during the pre-Harvey and post-Harvey cruises, however a time-history of four high quality
544 chlor-*a* images on August 18 (pre-Harvey), September 2 (6 days post-Harvey), September 11 and
545 September 16, 2017 (Fig. 7) revealed shelf events between the two cruises closest to Harvey's
546 landfall.

547

548 During mid-August, the highest chlorophyll-*a* concentrations and the maximum offshore extent
549 of blooms were found off central Louisiana, seaward and southwest of the Atchafalaya Bay
550 system, but within the 20m isobath. The zone of pigmented water extended to the 20 m isobath
551 southwest of Atchafalaya Bay but narrowed significantly from Sabine Lake (93.83°W) to Port
552 Aransas Bay (97°W). This distribution likely resulted from the pre-storm input of nutrients from
553 the Atchafalaya and Mississippi Rivers onto the shelf coupled with generally low summer flows
554 from Texas rivers. In contrast, by 2 September the highest chlorophyll-*a* concentrations were
555 detectable along the Texas coast between Sabine Lake and extending southwestwards to at least
556 Corpus Christi Bay. The widest zone of pigmented water extended well beyond the 20 m isobath
557 east, southeast, and south of Galveston Bay, likely due to the flux of nutrients and terrestrial



558

559 Fig. 8. Aqua-1 MODIS imagery depicting chlorophyll *a* estimates for August 18, September 2, September 11 and
560 September 16, 2017. White areas along the Louisiana shelf and offshore are clouds. Thin white lines denote 20m
561 and 100m isobaths. Station positions are indicated by the black dots on the 2 September image.

562

563 colored material from coastal areas flushed onto the shelf (Du et al., 2019). Maximum satellite-
564 derived coastal chlorophyll-*a* values near Galveston Bay were 16 mg m^{-3} . Moving seaward to
565 the 20 m isobath, values decreased to 10 mg m^{-3} and fell below 1 mg m^{-3} on the 100 m isobath
566 (Fig. 8). The accumulation of pigmented water with high chlorophyll-*a* concentrations between
567 Galveston Bay and Calcasieu Lake (93.45°W) likely resulted from convergence of the
568 downcoast Louisiana river waters (Quigg et al., 2011) with upcoast hurricane-related discharges
569 from the Galveston Bay region, as surface currents at TABS buoy B were offshore and decreased
570 from $\sim 75 \text{ cm/s}$ to 20 cm/s during the period from 30 August to 3 September (Fig. 3).

571

572 By September 11, the zone of pigmented water on the shelf near Galveston had retreated
573 shoreward and chlorophyll-*a* concentrations had decreased somewhat along the Texas coast,
574 while the highest concentrations were observed further east along the Louisiana coast near
575 Atchafalaya Bay (Fig. 8). Chlorophyll-*a* concentrations increased along the Texas coast by 16
576 September, accompanied by offshore movement in several lobes that reached the 100 m isobath



577 between Corpus Christi and the Mexican border at 26° N, but highest concentrations were only
578 about one tenth of those seen immediately after the storm. During the latter half of the month, the
579 maximum concentration of chlorophyll continued to decrease slowly and likely moved further
580 south and offshore under the influence of the prevailing currents (Fig. 3). Our first post-storm
581 cruise occurred between 22-27 September, so we would have missed the maximum extent of the
582 bloom and presumably also missed any offshore nutrient maximum that fueled the phytoplankton
583 growth. There was no evidence for upwelled nutrients resulting in blooms at the shelf edge, as
584 reported off Louisiana following Hurricane Ivan in 2004 (Walker et al., 2005) or in the East
585 China Sea by Chen et al. (2003).

586

587 In contrast to the satellite-derived data, fluorescence data from the CTD casts taken during all
588 cruises were much lower, especially in the upper mixed layer, where concentrations were
589 invariably $<1 \mu\text{g/L}$. During the period of the 22-27 September cruise measurements at only 4 of
590 37 stations had concentrations $>1.0 \text{ mg m}^{-3}$, while at 29 stations they were 0.5 mg m^{-3} or less.
591 The maximum concentration of 1.7 mg m^{-3} was found inshore just south of Galveston Bay.
592 Midwater maxima only exceeded 2 mg m^{-3} at offshore stations 27 and 28, where the maxima
593 were found at depths below 40m. This is similar to summer conditions reported by Nowlin et al.
594 (1998) and to previous data we have collected during summer cruises in the northern GoM.
595 Three days later, however, when the inshore stations were reoccupied, mean fluorescence values
596 showed $1\text{-}2 \text{ mg m}^{-3}$ at all inshore stations, with concentrations up to 4.8 mg m^{-3} immediately
597 offshore of Galveston in the plume. The steady wind conditions during the latter half of
598 September ($2\text{-}6 \text{ m/s}$ from the SE) may account for the difference between the two cruises, as
599 there was no mixing of the surface water and so only limited phytoplankton growth could take
600 place. As stated above, the discrepancy between satellite-derived and in situ values may be
601 related to CDOM interference in the satellite estimates, with the higher concentrations in early
602 September shown in Fig. 8 resulting at least partly from the hurricane stirring up bottom
603 sediments in the shallow coastal zone.

604

605 Although September is normally the month when seasonal hypoxia (oxygen concentrations <62
606 $\mu\text{mol/L}$) in the northern Gulf of Mexico ends, because of the passage of storm fronts, the strong
607 stratification resulting from the freshwater input might have been expected to reduce oxygen



608 concentrations below the pycnocline. Hypoxia in the northern Gulf of Mexico is generally
609 assumed to have three requirements: a high supply of nutrients, especially nitrogen, from rivers
610 or other terrestrial runoff, stable stratification with a mid-water pycnocline, and relatively low
611 wind conditions (Bianchi et al., 2010; Rabalais et al., 2007; Wiseman et al., 1997). This
612 combination of factors allows large phytoplankton populations to develop in the euphotic zone,
613 resulting in subpycnocline oxygen consumption during microbial respiration as the
614 phytoplankton die and sink. The presence of the pycnocline inhibits oxygen diffusion into the
615 bottom layer, resulting in oxygen depletion and eventually hypoxia, and relatively high
616 concentrations of organic matter can build up in the sediments, possibly leading to a reservoir of
617 labile material that contributes to hypoxia the following year during resuspension of the bottom
618 boundary layer (Hetland and DiMarco, 2008; Turner et al., 2008). Rabalais et al. (1999) state that
619 hypoxia can in fact occur in almost any month if conditions, particularly stratification, are right.
620 While the most intense hypoxia occurs over the Louisiana shelf (Rabalais et al., 1999), dissolved
621 oxygen levels below 30 $\mu\text{M/L}$ have been detected during NOAA SEAMAP cruises as far west as
622 96°W, with occasional samples between 30-60 $\mu\text{M/L}$ identified near Corpus Christi (see
623 <https://www.ncei.noaa.gov/maps/gulf-data-atlas/atlas.htm>), as well as following local flood
624 events (DiMarco et al., 2012; Kealoha et al., 2020), and bacteria from terrestrial sources have
625 been found in sponges at the Flower Gardens Banks National Marine Sanctuary near 28°N,
626 29.5°W (Shore et al., 2021).

627

628 Although hypoxia off the Texas coast has typically been linked to southwestward advection from
629 the Mississippi and Atchafalaya Rivers, high flow rates from local rivers have also been
630 implicated (Harper et al., 1981; Pokryfki and Randall, 1987; DiMarco et al., 2012). Di Marco et
631 al. (2012), using oxygen isotope data, specifically related hypoxia off the Brazos River mouth in
632 July 2007 to strong stratification following river discharge rates an order of magnitude higher
633 than normal. During the passage of Hurricane Harvey, the water column was completely mixed
634 and saturated in oxygen, but the torrential rainfall led to runoff that created a stable pycnocline,
635 and calm conditions after the storm meant that phytoplankton growth was possible. Further east,
636 on the Louisiana shelf, stratification is re-established within a few days of the passage of storm
637 fronts or hurricanes and bottom water oxygen depletion can begin rapidly once the storm has
638 passed (e.g., Bianchi et al., 2010; Jarvis et al., 2021). However, despite the strong stratification



639 observed along the Texas coast, the two particularly interesting points found following our
640 cruises were the lack of any obvious signs of hypoxia over the Texas shelf, and the apparent lack
641 of increased nutrient concentrations, other than phosphate, in coastal water following the passage
642 of the hurricane. Plotting the difference in salinity between surface and bottom samples, a
643 measure of water column stability (DiMarco et al., 2012), against bottom oxygen concentrations
644 during the September cruise gave only a low correlation, with $R^2 = 0.15$ ($n = 38$), as opposed to
645 the 0.79 ($n = 14$) reported in 2007 by DiMarco et al. (2012). This suggests that stratification by
646 itself was not responsible for the observed bottom oxygen concentrations over the shelf.

647

648 While hypoxia occurrence largely follows local nutrient supply, low oxygen waters can also be
649 injected onto the shelf from offshore through upwelling. Chen et al. (2003), for example,
650 suggested that hypoxia in the East China Sea could be induced by the “cross-shelf upwelling of
651 nutrient-rich Kuroshio water after the passage of typhoon Herb in a normally downwelling
652 region.” This led to increased primary productivity following the passage of the typhoon. While
653 they agreed with Shiah et al. (2000) that terrestrial runoff was a factor in increased local coastal
654 productivity following the storms, they suggested that the upwelling of subsurface Kuroshio
655 water was equally important. The increased upwelling was thought to result from “a larger
656 buoyancy effect caused by the rains as well as the shoreward movement of the Kuroshio caused
657 by the typhoons.”

658

659 The lack of hypoxia following Hurricane Harvey can therefore perhaps be explained by four
660 factors. First, only a limited flux of nutrients made it out of the bays and into the coastal zone,
661 where it was likely taken up rapidly by phytoplankton, as seen elsewhere. Additionally,
662 southward and offshore advection of low salinity runoff increased the rate of dilution through
663 mixing with pre-existing low-nutrient surface shelf water. The largest bay systems have
664 relatively narrow entrances, which reduce the rate at which the fresh water can escape – the main
665 entrance to Galveston Bay, which includes the deep, dredged Houston Ship Channel, is only 2.3
666 km wide and the turnover time for water is 15-60 days under normal conditions, with shorter
667 periods coinciding with flood conditions (Solis and Powell, 1999; Rayson et al., 2016). Thyng et
668 al. (2020) have estimated that the initial flushing of Galveston Bay during Hurricane Harvey
669 took only 2-3 days following the initial heavy rainfall. For the Corpus Christi Bay/Aransas Bay



670 system the turnover time under normal conditions is estimated to be more than 300 days (Solis
671 and Powell, 1999), similar to Pamlico Sound (Paerl et al., 2001).

672

673 Second, the sheer volume of water rapidly removed available soluble nutrients within the first
674 few hours so that runoff later during the storm was essentially pure rainwater. It is known that
675 large percentages of available nutrients are removed in stormwater runoff in the first minutes or
676 hours following a downpour and concentrations then drop (e.g., Cordery, 1977; Horner et al.,
677 1994; Fellman et al., 2008). Similar effects have been reported for trace metals in the floodplain
678 of the Pearl River in Mississippi (Shim et al., 2017), where maximum downstream
679 concentrations were not found following peak flows. These authors suggested that the rapid
680 flushing overwhelmed the rate at which soluble metal-organic complexes could be regenerated.
681 As the hurricane occurred in late summer, any nutrients applied to cropland along the Texas
682 coastline in spring would largely have been taken up by the vegetation and so be unavailable for
683 washout. While Corpus Christi (population ~325,000) and Houston (~4 million) are large
684 population centers with multiple sewage treatment plants that flooded following the hurricane,
685 both are sited upstream of large bay systems that would have attenuated the speed at which
686 stormwater runoff dissipated. The rate of change of nutrient concentrations in Galveston Bay
687 (Fig. 7) shows that uptake within the bay system was likely considerably more important than
688 flushing, even with the apparently short flushing time calculated by Thyng et al (2020).

689

690 While nutrient flushing was reduced following the hurricane, the same is unlikely to be true for
691 sediment. As shown in Fig. S2, and as discussed by D'Sa et al. (2018), Du et al. (2019), and
692 Steichen et al. (2020), large sediment plumes occurred off the mouths of major bays and rivers.
693 The heavy sediment loads would have not only increased the turbidity of the water column and
694 thereby reduced light intensity in the euphotic zone, but could also have led to reduced phosphate
695 concentrations as phosphate is known to bind to sediment particles (e.g., Suess, 1981). Both
696 factors would have contributed to reduced phytoplankton production, which is a major factor in
697 hypoxia formation (Bianchi et al., 2010). While phosphate concentrations in the coastal zone
698 were highest during the first September cruise, suggesting at least some terrestrial runoff
699 immediately following the hurricane and possibly desorption from suspended sediment, the low
700 nitrate concentrations seen during this cruise and the low chlorophyll fluorescence suggests only



701 a short-term phytoplankton bloom at most, again similar to previous observations (e.g., Roman et
702 al., 2005).

703

704 The final potential control is sediment composition along the Texas shelf. Most sediments in this
705 region are coarse, sandy, and contain little organic matter (Hedges and Parker, 1974). This is in
706 contrast to the Louisiana shelf, where muddy, organic sediments are quite common and act as a
707 reservoir of material that can continue to reduce oxygen concentrations once stratification is
708 established (Bianchi et al., 2010; Corbett et al., 2006; Eldridge and Morse, 2008; Turner et al.,
709 2008). This is especially true within coastal embayments, such as Terrebonne Bay, LA, where
710 the organic carbon content can exceed 5% thanks to organic matter input from the surrounding
711 marshes and swamps (Hedges and Parker, 1974; Bianchi et al., 2009, 2010). Even near the
712 Mississippi and Atchafalaya Rivers, however, typical organic carbon sediment content on the
713 shelf is generally <2% (Gordon and Goni, 2004; Gearing et al, 1977), while further west off the
714 Texas coast it is typically < 1% (Hedges and Parker, 1974, Bianchi et al., 1997). This suggests
715 that organic matter along the Texas shelf is refractory, and less likely to add to any oxygen
716 demand, and that hypoxia on the Texas shelf is generally driven by water column respiration as
717 discussed by Hetland and DiMarco (2008). In this region stratification alone is not sufficient to
718 bring about hypoxic conditions in the absence of high nutrient concentrations and phytoplankton
719 blooms.

720

721 **5 Conclusions**

722 Although Hurricane Harvey led to pronounced flooding and exceptional freshwater runoff along
723 the Texas coast, it did not lead to lasting high nutrient concentrations offshore, largely because of
724 dilution by the rainfall, and the likely rapid uptake by phytoplankton of nutrients washed out of
725 the bays. The most pronounced changes in nutrient concentrations were seen in the coastal bays.
726 Even here, changes from background levels were short-lived, and conditions were essentially
727 back to normal by November, some eight weeks after the hurricane, following northerly wind
728 bursts that caused mixing within the water column. While a transient bloom of phytoplankton
729 was observed in satellite imagery offshore following the hurricane, its short existence suggests
730 that hypoxia could not develop despite the stratification because nutrient concentrations were not
731 high enough to support continued phytoplankton productivity. Similarly, the lack of an organic



732 matter reservoir in the shelf sediments means there is no additional oxygen demand in Texas
733 bottom waters, and hypoxia here depends on water column decomposition.

734

735 **6 Acknowledgements**

736 We are grateful to the Captains and crews of the R.V. *Manta* and R.V. *Point Sur* for their
737 excellent service during the cruises, and to the enthusiasm of the students and technicians who
738 helped with data collection. The TABS system is funded by the Texas General Land Office and
739 operated by the TAMU Geochemical and Environmental Research Group. Cruises were funded
740 by the Texas Governor's Fund through the Texas OneGulf Center of Excellence and an NSF
741 RAPID award (OCE-1760381) to Drs. Knap, Chapman and DiMarco. A.H. K would also like to
742 acknowledge financial support from the G. Unger Vetlesen Foundation. We thank Ysabel Wang
743 for help with the figures, and Alaric Haag for assistance with SeaDAS image processing. Walker
744 and Haag thank the Gulf of Mexico Coastal Ocean Observing System (GCOOS) for funding
745 LSU Earth Scan Laboratory activities. Bathymetry shown in satellite imagery was provided by
746 GEBCO Compilation Group (2020) GEBCO 2020 Grid (doi:10.5285/a29c5465-b138-234d-
747 e053-6c86abc040b9). Funding sources had no involvement in study design, data collection and
748 interpretation, or manuscript preparation.

749

750 Data are being submitted to the Biological and Chemical Oceanography Data Management
751 Office (BCO-DMO). The title and DOI for the first set are: Processed CTD profile data from all
752 electronic sensors mounted on rosette from R/V Pt. Sur PS 18-09 Legs 01 and 03, Hurricane
753 Harvey RAPID Response cruise (western Gulf of Mexico) September-October 2017
754 (DOI:10.26008/1912/bco-dmo.809428.1).

755

756 **7 Credit author statement**

757 The project was conceptualized by SFD and AHK; PC and SFD conducted investigations on all
758 cruises and collected and analyzed the initial data; AQ provided data from Galveston Bay; NDW
759 provided satellite imagery. PC wrote the initial draft; all authors provided comments and edits.
760 The authors declare that they have no conflict of interest.

761



762 **References**

- 763 Ahn, J.H., Grant, S.B., Surbeck, C.Q., DiGiacomo, P.M., Nexlin, N., Jiang, S.: Coastal Water
764 Quality Impact of Stormwater Runoff from an Urban Watershed in Southern California.
765 *Environ. Sci. Technol.*, 39, 5940-5963, doi:10.1021/es0501464, 2005
- 766 Balaguru, K., Foltz, G.R., Leung, L.R.: Increasing magnitude of hurricane rapid intensification in
767 the central and eastern tropical Atlantic. *Geophys. Res. Lett.*, 45, 4238–4247, doi:
768 10.1029/2018GL077597, 2018
- 769 Bianchi, T.S., DiMarco, S.F., Smith, R.W., Schreiner, K.M.: A gradient of dissolved organic
770 carbon and lignin from Terrebonne-Timbalier Bay estuary to the Louisiana shelf (USA).
771 *Mar. Chem.*, 117, 32-41, doi: 10.1016/j.marchem.2009.07.010, 2009.
- 772 Bianchi, T.S., DiMarco, S.F., Cowan, J.H., Hetland, R.D., Chapman, P., Day, J.W.,
773 Allison, M.A.: The Science of Hypoxia in the Northern Gulf of Mexico: A Review.
774 *Sci. Total Environ.*, 408, 1471-1484; doi: 10.1016/j.scitotenv.2009.11.047, 2010.
- 775 Bianchi, T.S., Lambert, C.D., Santschi, P.H., Guo, L.: Sources and transport of land-derived
776 particulate and dissolved organic matter in the Gulf of Mexico (Texas slope/shelf): The use
777 of lignin-phenols and loliolides as biomarkers. *Org. Geochem.*, 27, 65-78, doi:
778 10.1016/S0146-6380(97)00040-5, 1997.
- 779 Blake, E.S., Zelinsky, D.A.: *Hurricane Harvey*. NOAA National Hurricane Center Tropical
780 Cyclone Report AL092017, 2018.
- 781 Chen, C-T. A., Liu, C-T., Chuang, W.S., Yang, Y.J., Shiah, F-K., Tang, T.Y., Chung, S.W.:
782 Enhanced buoyancy and hence upwelling of subsurface Kuroshio waters after a typhoon in
783 the southern East China Sea. *J. Mar. Sys.*, 42, 65-79, doi :10.1016/S0924-7963(03)00065-4,
784 2003.
- 785 Cochrane, J.D., Kelly F.J.: Low-frequency circulation on the Texas-Louisiana continental shelf.
786 *J. Geophys. Res.* 91, 10645-10659, doi: 10.1029/JC091iC09p10645, 1986.
- 787 Corbett, D.R., McKee, R.A., Allison, M.A.: Nature of decadal-scale sediment accumulation in
788 the Mississippi River deltaic region. *Cont. Shelf Res.*, 26, 2125-2140, doi:
789 10.1016/j.csr.2006.07.012, 2006.
- 790 Cordery, I.: Quality characteristics of urban storm water in Sydney, Australia. *Water Resources*
791 *Res.*, 13, 197-202, doi: 10.1029/WR013i001p00197, 1977.



- 792 De Carlo, E., Hoover, D.J., Young, C.W., Hoover, R.S., Mackenzie, F.T.: Impact of storm runoff
793 from tropical watersheds on coastal water quality and productivity. *Appl. Geochem.*, 22,
794 1777-1797. doi: 10.1016/j.apgeochem.2007.03.034, 2007.
- 795 DiMarco, S.F., Strauss, J., May, N., Mullins-Perry, R.L., Grossman, E. Shormann, D.: Texas
796 coastal hypoxia linked to Brazos River discharge as revealed by oxygen isotopes. *Aq.*
797 *Geochem.*, 18, 159-181, doi:10.1007/s10498-011-9156-x, 2012.
- 798 DiMarco, S.F., Zimmerle, H.M. 2017. *MCH Atlas: Oceanographic Observations of the*
799 *Mechanisms Controlling Hypoxia Project*. Texas A&M University, Texas Sea Grant
800 Publication TAMU-SG-17-601, 300 pp. (available online at <http://mchatlas.tamu.edu>).
- 801 D'Sa, E., Joshi, I., Liu, B.: Galveston Bay and coastal ocean optical-geochemical response to
802 Hurricane Harvey from VIIRS ocean color. *Geophys. Res. Lett.*, 45, 10,579-10,589
803 doi:10.1029/2018GL079954 2018.
- 804 Du, J., Park, K., Dellapenna, T.M., Clay, J.C.: Dramatic hydrodynamic and sedimentary
805 responses in Galveston Bay and adjacent inner shelf to Hurricane Harvey. *Sci. Total.*
806 *Environ.*, 653, 554-564, doi: 10.1016/j.scitotenv.2018.10.403, 2019.
- 807 Eldridge, P.M., Morse, J.W.: Origins and temporal scales of hypoxia on the Louisiana shelf:
808 importance of benthic and sub-pycnocline water column metabolism. *Mar. Chem.*, 108, 159-
809 171, doi: 10.1016/j.marchem.2007.11.009, 2008.
- 810 Emanuel, K.: Assessing the present and future probability of Hurricane Harvey's
811 rainfall. *Proc. Natl. Acad. Sci. U.S.A.*, 114, 12681–12684, doi:10.1073/
812 pnas.1716222114, 2017.
- 813 Fellman, J.B., Hood, E., Edwards, R.T., D'Amore, D.V.: Return of salmon-derived nutrients
814 from the riparian zone to the stream during a storm in southeastern Alaska. *Ecosystems*, 11,
815 537-544, doi: 10.1007/s10021-008-9139-y, 2008.
- 816 Fritz, A., Samenow, J. 2017. Harvey Unloaded 33 Trillion Gallons of Water in the U.S. The
817 Washington Post, September 2, 2017. <https://www.washingtonpost.com/news/capital-weather-gang/wp/2017/08/30/harvey-has-unloaded-24-5-trillion-gallons-of-water-on-texas-and-louisiana/>.
- 818
819
- 820 Gearing, P., Plucker, F.T., Parker, P.L.: Organic carbon stable isotope ratios of continental
821 margin sediments. *Mar. Chem.*, 5, 251-266, doi: 10.1016/0304-4203(77)90020-2, 1977.



- 822 Gilbes, F., Armstrong, R.A., Webb, R.M.T., Muller-Karger, F.E.: SeaWiFS helps assess
823 hurricane impact on phytoplankton in Caribbean Sea. *Eos, Trans. Amer. Geophys. Union*, 82,
824 529, 533, doi: 10.1029/01EO00314, 2001.
- 825 Gordon, E.S., Goni, M.A.: Controls on the distribution and accumulation of terrigenous organic
826 matter in sediments from the Mississippi and Atchafalaya river margin. *Mar. Chem.*, 92, 331-
827 352, doi: 10.1016/j.marchem.2004.06.035, 2004.
- 828 Harper, D.E. Jr., Salzer R.R., Case R.J.: The occurrence of hypoxic bottom water off the upper
829 Texas coast and its effect on the benthic biota. *Contr. Mar. Sci.*, 24, 53-79, 1981.
- 830 Hedges, J.I. , Parker, P.L.: Land-derived organic matter in surface sediments from the Gulf of
831 Mexico. *Geochim. Cosmochim. Acta*, 40, 1019-1029, doi: 10.1016/0016-7037(76)90044-2,
832 1974.
- 833 Hetland, R.D., DiMarco, S.F.: How does the character of oxygen demand control the structure of
834 hypoxia on the Texas-Louisiana continental shelf? *J. Mar. Sys.*, 70, 49-62, doi:
835 10.1016/j.jmarsys.2007.03.002, 2008.
- 836 Horner, R. R., Skupien, J. J., Livingston, E. H., and Shaver, H. E.: *Fundamentals of urban runoff*
837 *management: Technical and institutional issues*. Terrene Institute, Washington, D.C., 1994.
- 838 Jarvis, B.M., Greene, R.M., Wan, Y., Lehrter, J.C., Lowe, L.L., Ko, D.S: Contiguous low
839 oxygen waters between the continental shelf hypoxia zone and nearshore coastal waters of
840 Louisiana, USA: interpreting 30 years of profiling data and three-dimensional ecosystem
841 modeling. *Environ. Sci. Technol.*, 55, 4709-4719, doi: 10.1021/acs.est.0c05973, 2021.
- 842 Kealoha, A.K., Doyle, S.M., Shamberger, K.E.F., Sylvan, J.B., Hetland, R.D., DiMarco, S.F.:
843 Localized hypoxia may have caused coral reef mortality at the Flower Garden Banks. *Coral*
844 *Reefs*, 39, 119-132, doi: 10.1007/s00338-019-01883-9, 2020.
- 845 Larson, E. 1999. *Isaac's Storm*. Random House, New York, 323 pp, ISBN 0-609-60233-0.
- 846 Liu, B., D'Sa, E., Joashi, I.: Floodwater impact on Galveston Bay phytoplankton taxonomy,
847 pigment composition and photo-physiological state following Hurricane Harvey from field
848 and ocean color (Sentinel-3A OLCI) observations. *Biogeosci.*, 16, 1975-2001;
849 doi:10.5194/bg-2018-504, 2019.
- 850 Mallin, M.A., Corbett, C.A.: How hurricane attributes determine the extent of environmental
851 effects: multiple hurricanes and different coastal systems. *Estuar. Coasts.*, 29, 1046-1061,
852 doi: 10.1007/BF02798667, 2006.



- 853 Montagna, P., Hu, X., Walker, L., Wetz, M. 2017. Biogeochemical impact of Hurricane Harvey
854 on Texas coastal lagoons. AGU Fall Meeting Abstract #NH23E-2797.
- 855 Nowlin, W.D.Jr., Jochens, A.E., Reid, R.O., DiMarco, S.F. 1998. Texas-Louisiana Shelf
856 Circulation and Transport Processes Study: Synthesis Report. *PCS Study MMS 98-0035*. U.S.
857 Department of the Interior, Minerals Management Service, Gulf of Mexico OCS Region,
858 New Orleans, LA.
- 859 Paerl, H.W., Bales, J.D., Ausley, L.W., Buzzelli, C.P., Crowder, L.B., Eby, L.A., Fear, J.M., Go,
860 M., Peierls, B.L., Richardson, T.L., Ramus, J.S.: Ecosystem impacts of three sequential
861 hurricanes (Dennis, Floyd, and Irene) on the United States' largest lagoonal estuary,
862 PamlicoSound, NC. *Proc. Natl. Acad. Sci. U.S.A.*, 98, 5655–5660, doi:
863 10.1073/pnas.101097398, 2001.
- 864 Paerl, H.W., Crosswell, J.R., Van Dam, B., Hall, N.S., Rossignol, K.L., Osburn, C.L., Hounshell,
865 A.G., Sloup, R.S., Harding, L.W. Jr.: Two decades of tropical cyclone impacts on North
866 Carolina's estuarine carbon, nutrient and phytoplankton dynamics: implications for
867 biogeochemical cycling and water quality in a stormier world. *Biogeochem.*, doi:
868 10.1007/s10533-018-0438-x, 2018.
- 869 Paerl, H.W., Valdes, L.M., Joyner, A.R., Peierls, B.L., Piehler, M.F., Riggs, S.R., Christian,
870 R.R., Eby, L.A., Crowder, L.B., Ramus, J.S., Clesceri, E.J., Buzzelli, C.P., Luettich, R.A.:
871 Ecological response to hurricane events in the Pamlico Sound system, North Carolina, and
872 implications for assessment and management in a regime of increased frequency. *Estuar.*
873 *Coasts*, 29, 1033–1045, doi:10.1007/BF02798666, 2006.
- 874 Peierls, B.L., Christian, R.R., Paerl, H.W.: Water quality and phytoplankton as indicators of
875 hurricane impacts on a large estuarine system. *Estuar.*, 26, 1329-1343, doi:
876 10.1007/BF02803635, 2003.
- 877 Pokryfki, L., Randall, R.E.: Nearshore hypoxia in the bottom water of the northwestern Gulf of
878 Mexico from 1981 to 1984. *Mar. Environ. Res.*, 22, 75-90, doi: 10.1016/0141-
879 1136(87)90081-X, 1987.
- 880 Potter, H., DiMarco, S.F., Knap, A.H.: Tropical cyclone heat potential and the rapid
881 intensification of hurricane Harvey in the Texas Bight. *J. Geophys. Res. (Oceans)*, 124,
882 2440-2451, doi:10.1029/2018JC014776, 2019.



- 883 Quigg, A., Sylvan, S.B., Gustafson, A.B., Fisher, T.R., Oliver, R.L., Tozzi, S., Ammerman, J.W.:
884 Going West: nutrient limitation of primary production in the northern Gulf of Mexico and the
885 importance of the Atchafalaya River. *Aq. Geochem.*, 17, 519-544, doi: 10.1007/s10498-011-
886 9134-3, 2011.
- 887 Rabalais, N.N., Turner, R.E., Justic, D., Dortch, Q., Wiseman, W.J., Jr.: Characterization of
888 Hypoxia: Topic 1 Report for the Integrated Assessment of Hypoxia in the Gulf of Mexico.
889 NOAA Coastal Ocean Program Decision Analysis Series No. 15. NOAA Coastal Ocean
890 Program, Silver Spring, Maryland, 1999.
- 891 Rabalais, N.N., Turner, R.E., Sen Gupta, B.K., Boesch, D.F., Chapman, P., Murrell, M.C.:
892 Hypoxia in the northern Gulf of Mexico: Does the science support the plan to reduce,
893 mitigate and control hypoxia? *Estuar. Coasts*, 30, 753-772, doi: 10.1007/BF02841332, 2007.
- 894 Rayson, M.D., Gross, E.S., Hetland, R.D., Fringer, O.B.: Time scales in Galveston Bay: an
895 unsteady estuary. *J. Geophys. Res. (Oceans)*, 121, 2268-285, doi: 10.1002/2015JC011181,
896 2016.
- 897 Roman, M.R., Adolf, J.E., Bichy, J., Boicourt, W.C., Harding, L.W., Houde, E.D., Jung, S.,
898 Kimmel, D.G., Miller, W.D., Zhang, X.: Chesapeake Bay plankton and fish abundance
899 enhanced by Hurricane Isabel. *EOS*, 86, 261-265, doi: 10.1029/2005EO280001, 2005.
- 900 Sahl, L.E., Merrell, W.J., Biggs, D.C.: The influence of advection on the spatial variability of
901 nutrient concentrations on the Texas-Louisiana continental shelf. *Cont. Shelf. Res.*, 13, 233-
902 251; doi: 10.1016/0278-4343(93)90108-A, 1993.
- 903 Shiah, F.K., Chang, S.W., Kao, S.J., Gong, G.C., Liu, K.K.: Biological and hydrographical
904 responses to tropical cyclones (typhoons) in the continental shelf of the Taiwan Strait. *Cont.*
905 *Shelf. Res.*, 20, 2029-2044, doi: 10.1016/S0278-4343(00)00055-8, 2000.
- 906 Shim, M.J., Cai, Y., Guo, L., Shiller, A.M.: Floodplain effects on the transport of dissolved and
907 colloidal trace elements in the East Pearl River, Mississippi. *Hydrol Proc.*, 31, 1086-1099,
908 doi: 10.1002/hyp.11093, 2017.
- 909 Shore, A., Sims, J.A., Grimes, M., Howe-Kerr, L.I., Grupstra, C.G.B., Doyle, S.M., Stadler, L.,
910 Sylvan J.B., Shamberger, K.E.F., Davies, S.W., Santiago-Vazquez, L.Z., Correa, A.N.S.: On
911 a reef far, far away: Anthropogenic impacts following extreme storms affect sponge health
912 and bacterial communities. *Front. Mar. Sci.*, 8: 608036, doi: 10.3389/mars.2021.608036,
913 2021.



- 914 Solis, G.S., Powell, G.L. : Hydrography, mixing characteristics, and residence times of Gulf of
915 Mexico estuaries. In: Bianchi, T.S., Pennock, J.R., Twilley, R.R. (eds). *Biogeochemistry of*
916 *Gulf of Mexico Estuaries*, John Wiley, NY, pp. 29-61, 1999.
- 917 Steichen, J.L., Labonte, J.M., Windham, R., Hala, D., Kaiser, K., Setta, S., Faulkner, P.C.,
918 Bacosa, H., Yan, G., Kamalanathan, M., Quigg, A.: Microbial, physical and chemical
919 changes in Galveston Bay following an extreme flood event, Hurricane Harvey. *Front. Mar.*
920 *Sci.*, 7, 186, doi:10.3389/fmars.2020.00.00186, 2020.
- 921 Suess, E.: Phosphate regeneration from sediments of the Peru continental margin by dissolution
922 of fish debris. *Geochem. Cosmochim. Acta*, 45, 577-588, doi: 10.1016/0016-7037(81)90191-
923 5, 1981.
- 924 Sylvan, J.B., Dortch, Q., Nelson, D.M., Brown, A.F.M., Morrison, W., Ammerman, J.W.:
925 Phosphorus limits phytoplankton growth on the Louisiana shelf during the period of hypoxia
926 formation. *Environ. Sci. Tech.*, 40, 7548-7553, doi : 10.1021/es061417t, 2006.
- 927 Sylvan, J.B., Quigg, A., Tozzi, S., Ammerman, J.W. : Eutrophication induced phosphorus
928 limitation in the Mississippi River plume: evidence from fast repetition rate fluorometry.
929 *Limnol. Oceanogr.*, 52, 2679-2685, doi: 10.4319/lo.2007.52.6.2679, 2007.
- 930 Thyng, K.M., Hetland, R.D., Socolofsky, S.A., Fernando, N., Turner, E.L., Schoenbaechler, C.:
931 Hurricane Harvey caused unprecedented freshwater inflow to Galveston Bay. *Estuar. Coasts*,
932 doi:10.1007/s12237-020-00800-6, 2020.
- 933 Trenberth K.E., Chang L., Jacobs P., Zhang Y., Fasullo, J.: Hurricane Harvey links to ocean heat
934 content and climate change adaptation. *Earth's Future* 6, 730-744, doi:
935 10.1029/2018EF000825, 2018.
- 936 Turner R.E., Rabalais N.N., Justic D.: Gulf of Mexico Hypoxia: Alternate States and a Legacy.
937 *Environ. Sci. Technol.*, 42, 2323–2327, doi:10.1021/es071617k, 2008.
- 938 Walker, L.M., Montagna, P.A., Hu, X., Wetz, M.S.: Timescales and magnitude of water quality
939 change in three Texas estuaries induced by passage of Hurricane Harvey. *Estuar. Coasts*, 44,
940 960-971, doi: 10.1007/s12237-020-00846-6, 2021.
- 941 Walker, N.D.: Wind and eddy-related shelf/slope circulation processes and coastal upwelling in
942 the Northwestern Gulf of Mexico. In: Sturges W, Lugo-Fernandez A, editors. *Circulation in*
943 *the Gulf of Mexico: Observations and Models. Geophys. Monographs* 161, American
944 Geophysical Union, 295-313, doi:10.1029/161GM21, 2005.



- 945 Walker, N.D., Leben, R.R., Balasubramanian, S.: Hurricane-forced upwelling and chlorophyll *a*
946 enhancement within cold-core cyclones in the Gulf of Mexico. *Geophys. Res. Lett.* 32,
947 doi:10.1029/2005GL023716, 2005.
- 948 WHPO. 1994. *WHP Operations and Methods*. WOCE Hydrographic Office Report 91/1, as
949 revised, WOCE Hydrographic Programme Office, Woods Hole, MA.
- 950 Wiseman, W.J., Rabalais, N.N., Turner, R.E., Dinnel, S.P., McNaughton, A.: Seasonal and
951 interannual variability within the Louisiana coastal current: stratification and hypoxia. *J.*
952 *Mar. Sys.*, 12, 237-248, doi: 10.1016/S0924-7963(96)00100-5, 1997.
- 953 Zhang, J.-Z., Kelbie, C.R., Fischer, C.J., Moore, L.: Hurricane Katrina induced nutrient runoff
954 from an agricultural area to coastal waters in Biscayne Bay, Florida. *Est. Coastal Shelf Sci.*,
955 84, 209-218, doi: 10.1016/j.ecss.2009.06.026, 2009.
- 956